https://doi.org/10.22226/2410-3535-2021-3-315-320 PACS: 81.05.-t; 81.15.Cd

Effect of alloying with Cu and TiN addition on the electrochemical behavior of nanocrystalline Ni processed by magnetron sputtering

Mukesh Kumar

mukesh.kumar@sgtuniversity.org

Department of Physics, Faculty of Science, Shree Guru Gobind Singh Tricentenary University, Gurgaon, Delhi-NCR, 122001, India

Electrochemical behavior of the nanocomposite coatings plays an important role in order to side their applications in protective coatings either on the different tools used in automobile as well as aerospace industries or on engineering materials. For this purpose, nanocrystalline Ni, $Ni_{90}Cu_{10}$, Ni-TiN and $Ni_{90}Cu_{10}$-TiN thin films have been deposited by reactive magnetron co-sputtering on silicon substrate. Grain sizes and the phases present in the processed films have been analyzed by using a grazing incident X-ray diffraction pattern. The average grain sizes are measured to be around 13.6 ± 0.4 nm for Ni and 9.6 ± 0.3 nm for TiN. Microstructural and elemental analyses of the investigated samples before and after the electrochemical tests have been done by field emission scanning electron microscopy and an energy dispersive X-ray analyzer, respectively. Microstructure for pure Ni films reveals the formation of pits on the surface after electrochemical test. Furthermore, the electrochemical behaviour of these thin films has been investigated with the help of potentiodynamic polarization experiments. Nanocrystalline Ni films are found to be more susceptible for pitting corrosion. Further, resistance for pitting corrosion is found to increase with alloying with Cu as well as TiN addition in Ni matrix. Formation of TiO_2 protective layer has been confirmed by X-ray photo electron microscopy (XPS).

Keywords: reactive magnetron co-sputtering, nanocomposite coatings, microstructure, XPS, electrochemical behaviour.

УДК: 538.9

Влияние легирования Cu и TiN на электрохимическое поведение нанокристаллического Ni, полученного магнетронным распылением

Мукеш Кумар

Кафедра физики, факультет естественных наук, Трехсотлетний университет Шри Гуру Гобинд Сингха, Гургаон, Дели-Национальный столичный регион, 122001, Индия

Электрохимическое поведение нанокомпозитных покрытий играет важную роль, поскольку они используются в качестве защитных покрытий на различных инструментах, используемых в автомобильной и аэрокосмической промышленности, или на конструкционных материалах. С этой целью нанокристаллические тонкие пленки Ni, $Ni_{90}Cu_{10}$, Ni-TiN и $Ni_{90}Cu_{10}$-TiN были нанесены реактивным магнетронным со-распылением на кремниевую подложку. Размеры зерен и фазы, присутствующие в обработанных пленках, были проанализированы с использованием картины дифракции рентгеновских лучей при скользящем падении. Средний размер зерна составляет около 13.6 ± 0.4 нм для Ni и 9.6 ± 0.3 нм для TiN. Микроструктурный и элементный анализы исследуемых образцов до и после электрохимических испытаний были выполнены с помощью автоэмиссионной сканирующей электронной микроскопии и энергодисперсионного рентгеновского анализатора соответственно. Микроструктура пленок чис-

того Ni показывает образование ямок на поверхности после электрохимических испытаний. Кроме того, электрохимическое поведение этих тонких пленок было исследовано с помощью экспериментов по потенциодинамической поляризации. Обнаружено, что нанокристаллические пленки Ni более подвержены питтинговой коррозии. Кроме того, обнаружено, что стойкость к питтинговой коррозии увеличивается при легировании Cu, а также добавлении TiN в матрицу Ni. Образование защитного слоя TiO_2 подтверждено рентгеновской фотоэлектронной микроскопией (XPS).

Ключевые слова: реактивное магнетронное сораспыление, нанокомпозитные покрытия, микроструктура, XPS, электрохимическое поведение.

1. Introduction

Nickel-based nanocomposite coatings have got significant notice world-wide because of their interesting applications such as protective coatings on the different tools used in automobile as well as aerospace industries and on engineering materials due to their high corrosion resistance, as well as reasonably high elastic modulus and hardness. A literature survey reports on the existing works related to the Ni-based nanocomposite as well as alloys films [1–17] show that several investigations have been done on processing, microstructure and associated properties of the electrodeposited nanocomposite coatings such as Ni-ZrO_2 [3], Ni-SiC [4, 5], Ni-Al_2O_3 [7], and Ni-TiN [8]. Furthermore, Balathandan et al. [18] have found that the Ni matrix nanocomposite films reinforced with nano-size CeO_2, ZrO_2, Al_2O_3, TiN and La_2O_3 particles possess better corrosion resistance as compared to pure Ni coatings. It has been also reported that Ni-SiC nanostructured composite coatings processed by the electrodeposition technique exhibit better resistance to corrosion as compared to pure Ni [2]. The electrochemical behavior of the Ni-TiN nanocomposite film in the 3.5% NaCl solution, has been observed to be superior than the pure Ni films [8]. Of course, further research is required to understand the operative mechanism for protection against corrosion in Ni-based nanocomposite coatings. Another problem is that despite of inexpensive electrodeposition coatings process, there is a possibility of contamination of grown films due to presence of electrolytic constituents and other reagents. However, for the processing of nanocomposite coatings with appropriate composition, magnetron sputtering technique can be considered as promising alternative. The details of magnetron sputter deposition technique and effect of processing parameters on microstructure and properties of Ni-TiN nanocomposite thin films have been studied in-depth by Mukesh et. al [19 – 21]. Most recently, Bibhu et al. [22] have studies the electrochemical behavior of $Ni_{1-x}Ti_xN$ nanocomposite films in 3.5 wt.% NaCl solution. There has been observed to be improvement in corrosion resistance of $Ni_{1-x}Ti_xN$ nanocomposite films as compared to pure Ni films due to the formation of nanometric dispersoids of TiN in nickel matrix. In the present investigation, a systematic study has been done on the formation of nanocrystalline Ni, $Ni_{90}Cu_{10}$, Ni-TiN and $Ni_{90}Cu_{10}$-TiN nanocomposite thin films processed by reactive magnetron co-sputtering. Further, microstructural analysis and corrosion behavior of these films have been examined and compared.

2. Experimental procedure

2.1. Processing

The investigated thin films were processed by a magnetron sputtering system (model KVS-T 4065) under nitrogen plus argon gas environment. This system was equipped with two DC power sources and one RF power source for sputtering. Before sputtering of target materials (Ni, Cu and Ti with 99.9% purity), the chamber was evacuated to a base pressure lower than 2×10^{-6} Torr using a rotary pump and a turbo-molecular pump. During sputtering, Ar to N_2 gas ratio was controlled by a throttle valve and an MKS Baraton gauge was used for monitoring the chamber pressure. The thin films were deposited on ultrasonically cleaned (first in acetone and then isopropanol) p-type Si (100) substrates. Furthermore, for maintaining the compositional uniformity, the substrates were rotated at 25 rpm. The parameters used for deposition of the investigated thin films are shown in Table 1.

Table 1. Parameters used during the processing of the investigated films.

Processing parameters	Values
Base pressure	2.0×10^{-6} Torr
Working pressure	30 mTorr
Ar:N2	1:2
Ti RF Power	300 W
Ni DC Power	50 W
Cu DC Power	9 W
Substrate temperature	RT
Substrate bias	−60 V
Substrate Rotation Speed	25 rpm
Distance between Substrate and Target	150 mm

2.2. Characterization

The thicknesses of the as-deposited films were measured using a surface profilometer (Dektak 150, USA). The grain sizes and the phases present in the investigated films have been measured by using grazing incidence X-ray diffraction (GIXRD) (Philips X'Pert PRO Diffractometer, Netherlands, 40 K accelerating voltage and 30 mA current) using Cu-K_α radiation. The GIXRD scans were performed at grazing angle of 1.5°, in the range between 35° and 65°, at a scanning speed of 0.05°/s. The microstructures and element present in the thin films were investigated using a field emission scanning electron microscope (FESEM) (Zeiss SUPRA 40, Germany) and an energy dispersive X-ray

(EDX) microanalyzer, respectively. The electrochemical behaviour was investigated with the help of Autolab PG Stat-30 (Petentiostat/Galvanostat) corrosion measurement system controlled by a personal computer. All the corrosion tests were performed in 3.5% NaCl solution with pH ≈ 6.7 at room temperature. The standard three electrode system, with a platinum wire as a counter electrode, silver/silver chloride electrode (Ag/AgCl) as reference electrode and the sample as a working electrode (area: 1 cm^2) were employed in the present investigation. To analyze the formation of protective layer on the films, X-ray photoelectron spectroscopy (Model: PHI 5000 Versa Probe II) was carried out at the acceleration voltage of 15 kV in a chamber with base vacuum of ≈10^{-8} Torr using Al-K_α (1.487 KeV) radiation as the excitation source with beam size of ≈100 μm^2.

3. Results

The X-ray diffraction patterns of Ni, $Ni_{90}Cu_{10}$, Ni-TiN, and $Ni_{90}Cu_{10}$-TiN thin films processed by magnetron co-sputtering under optimized conditions have been presented in Fig. 1. This shows shift in the Ni peak positions towards the lower 2θ angle leads to the increase in lattice constant due to the formation of $Ni_{90}Cu_{10}$ alloys thin films. The average grain sizes of the Ni matrix and TiN calculated from the XRD peak widths using Scherer's equation [23] are found to be around 13.6 ± 0.4 nm and 9.6 ± 0.3 nm. The values of grain size are also found to decrease marginally either with alloying or with addition of TiN as reinforcement in the Ni matrix.

The typical FESEM micrographs depicting the microstructure of Ni, $Ni_{90}Cu_{10}$, Ni-TiN and $Ni_{90}Cu_{10}$-TiN nanocomposite films are shown in Fig. 2 a, b, c, and d, respectively. As shown in Fig. 2 a – d, the microstructures of each of the investigated films appear to be granular and dense.

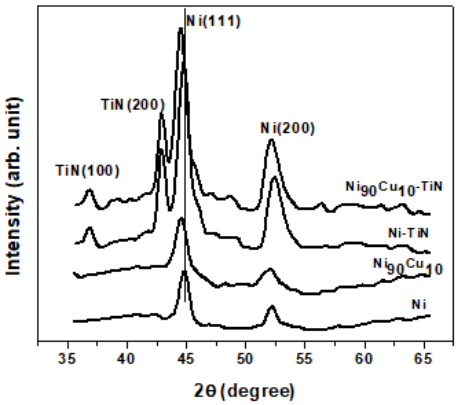

Fig. 1. XRD patterns of nanocrystalline Ni, $Ni_{90}Cu_{10}$, Ni-TiN, and $Ni_{90}Cu_{10}$-TiN nanocomposite thin films deposited under optimized conditions.

The potentiodynamic polarization curves obtained by subjecting thin films to corrosion tests in 3.5 g/l NaCl solution are shown in Fig. 3. The quantitative information on corrosion current density (I_{corr} in A/cm^2) and corrosion potential (E_{corr} in Volts) can be extracted from the intersection of the slopes of the potentiodynamic linear polarization curves [24], using the Stern-Geary equation [25].

The corrosion rate can be calculated using the following relation:

$$\text{Corrosion rate (mm/year)} = I_{corr} \cdot M \cdot C / D \cdot V_l, \qquad (1)$$

where, I_{corr} (A/cm^2) is the current density, D (g/cm^3) is the density of the sample, M (g) is the gram atomic mass, V_l is the valence and C is the Faraday constant. The electrochemical parameters obtained from the potentiodynamic polarization curves are shown in Table 2.

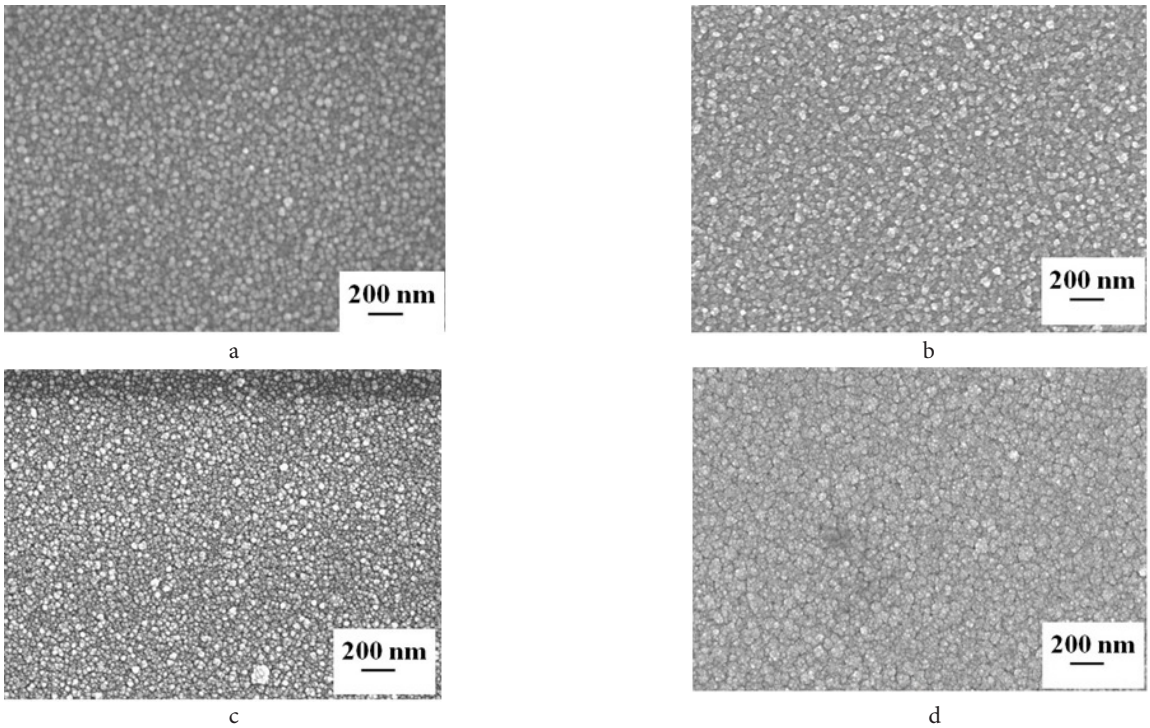

Fig. 2. FESEM micrographs depicting the microstructure of: Ni film (a), $Ni_{90}Cu_{10}$ alloy film (b), Ni-TiN nanocomposite film (c) and $Ni_{90}Cu_{10}$-TiN nanocomposite films (d).

From the results depicted in Table 2, it is observed that the corrosion rates in 3.5 g/l NaCl solution decrease in the following order: Ni < $Ni_{90}Cu_{10}$ < Ni-TiN < $Ni_{90}Cu_{10}$-TiN. This trend indicates that the corrosion resistance of pure Ni is improved on addition of TiN as reinforcement, as well as on alloying of the Ni matrix with Cu.

The corroded surfaces of Ni, $Ni_{90}Cu_{10}$, as well as Ni-TiN and $Ni_{90}Cu_{10}$-TiN nanocomposite films have been examined using FESEM along with EDX analyses to understand the mechanism of degradation. The FESEM images depicting the corroded surfaces of the presently investigated thin films subjected to potentiodynamic polarization tests are shown in Fig. 4. shows that the corroded surfaces of nanocrystalline Ni presented in Fig. 4a and $Ni_{90}Cu_{10}$ film presented in Fig. 4b contains large pits, whereas the images representing Ni-TiN in Fig. 4c and $Ni_{90}Cu_{10}$-TiN nanocomposite thin films in Fig. 4d do not show pits. Of course, the surface of the $Ni_{90}Cu_{10}$ film shows relatively fewer pits compared to that observed on the Ni surface. The EDX analysis of the corroded surfaces being investigated in this study has show evidence for significant enrichment of O. Furthermore, the results of XPS study as shown in Fig. 5. confirm the formation of TiO_2 on the surface of the nanocomposite thin film, which probably acts as a passive layer to protect the film from further degradation. The chemical reaction leading to the formation of TiO_2 as a passive layer is:

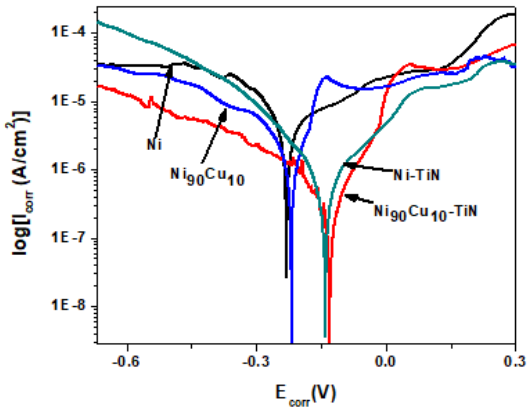

Fig. 3. (Color online) Potentiodynamic polarization curves of the investigated thin films in 3.5 g/l NaCl solution.

$$TiN + 2H_2O \rightarrow TiO_2 + 0.5N_2 + 4H^+ + 4e^-. \qquad (2)$$

The enhancement of corrosion resistance with increase in volume fraction of TiN could be attributed to the formation of passive layer of TiO_2, as confirmed by XPS analyses presented in Fig. 5.

Table 2. The electrochemical parameters obtained from the corrosion tests on the thin films of in 3.5 g/l NaCl solution.

Samples	E_{corr} (V)	I_{corr} (A/cm²)×10⁻⁶	R_p (Ω) × 10³	Corrosion rate (mm/yr) ×10⁻²
Ni	−0.230	1.55	1.01	1.67
$Ni_{90}Cu_{10}$	−0.206	1.05	4.7	0.92
Ni-TiN	−0.140	0.44	14.18	0.19
$Ni_{90}Cu_{10}$-TiN	−0.128	0.18	18.29	0.08

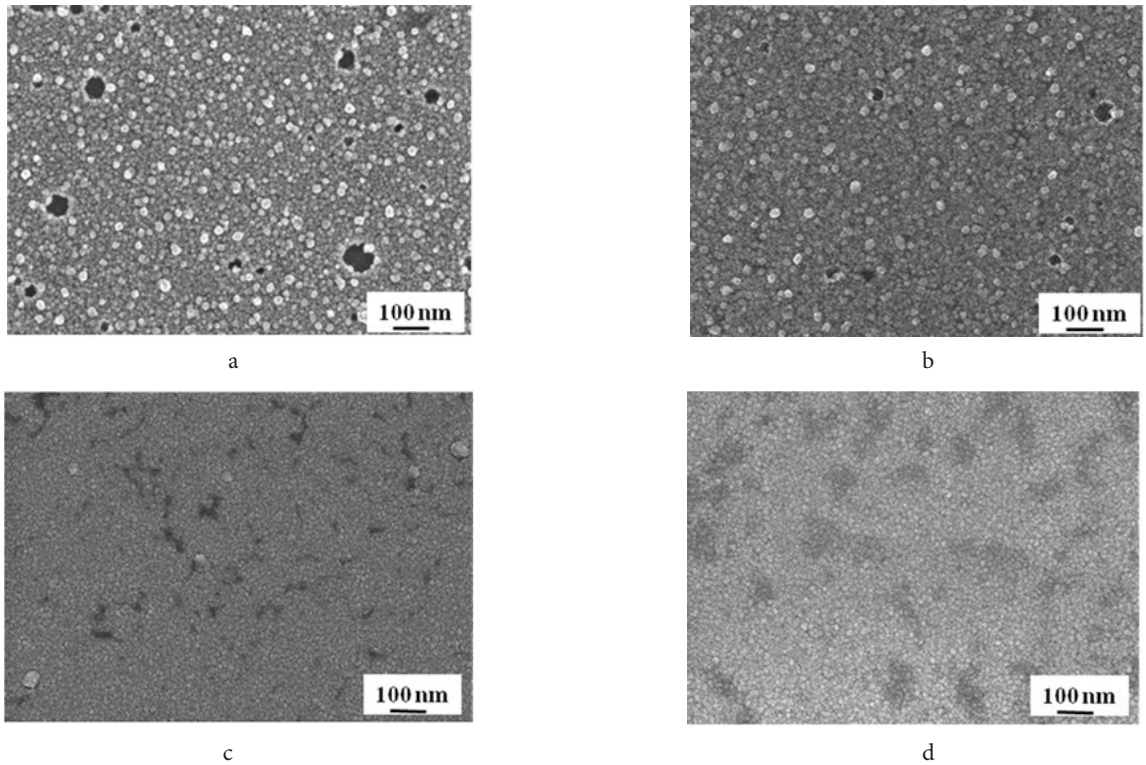

Fig. 4. FESEM (SE) micrographs of the corroded surfaces of the thin films of: Ni film (a), $Ni_{90}Cu_{10}$ alloy film (b), Ni-TiN nanocomposite film (c) and $Ni_{90}Cu_{10}$-TiN nanocomposite films (d).

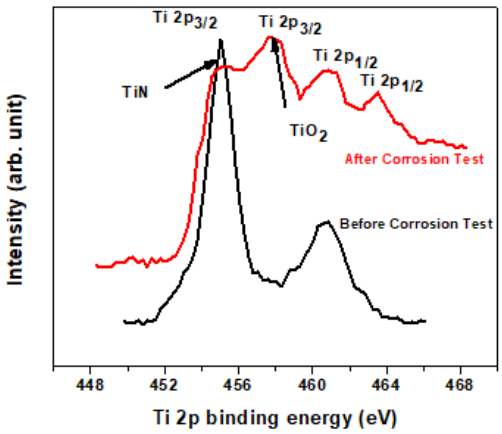

Fig. 5. (Color online) Ti 2p peaks in the XPS spectra from the surface of the Ni-TiN nanocomposite film before and after the corrosion test.

4. Discussion

4.1. Selection of the target power and deposition time

The target powers selection for this study has been based on the outputs of the optimization experiments made to evaluate the growth rates of Ti, Ni and Cu films by sputtering independently at different powers in Ar atmosphere. In addition to that, the effect of Ti (RF) target power on the growth rate of TiN film has been also examined in $Ar + N_2$ gas environment. From these experiment, it has been observed that the sputter yield of Ni (DC) target and Cu (DC) target are much higher than that of Ti (RF) target power. Therefore, on the basis of these experiment the Ni (DC), Cu (DC) and Ti (RF) target powers have been selected. Moreover, the combination of target powers and duration of deposition have been selected to obtain films thicknesses higher than 500 nm, so that during the corrosion experiments, the films could not be completely consumed or detachment from the substrate.

4.2. Corrosion mechanism and protection

Nanocrystalline Ni films has been found to be prone to pitting corrosion when exposed to 3.5 g/l NaCl solution, as shown in Fig. 4 a. Pure Ni is known to form a passive layer of $Ni(OH)_2$ in de-aerated water [26]. The mechanism of pitting corrosion in general has been well-documented [27]. Furthermore, the pitting corrosion resistance of nanocrystalline metallic samples has been found to increase with decrease in grain size. Through a study on the electrodeposited Ni films, it has been shown that besides grain size, morphology also has a significant effect on the corrosion behavior, with rough locations being more susceptible [28]. Moreover, the preferred orientation of Ni <111> is also expected to enhance pitting corrosion, as suggested by an earlier study by Tokuda and Ives [29].

In the Ni-Cu alloys, Ni is more reactive than Cu according to the emf series. As Cu resists pitting, it is intuitive that its addition as alloying element to Ni would enhance the resistance to pitting corrosion. The presence of Cu as alloying element is known to cause the formation of a passive layer of Cu_2O [30], which protects against further corrosion. Pitting corrosion in Ni-Cu alloy involving selective dissolution of Ni has been reported for Monel-400 alloy, leading to enrichment of Cu, at the expense of Ni inside the pits [31]. Furthermore, depletion of O along with enrichment of Cl- inside the pit with respect to that at the surrounding surface has been observed. It has been proposed that the presence of Cl^- anions increases the potential difference across the passive film of Cu_2O, which in turn increases the rate of Ni^+ ion diffusion from the Ni-film interface to the film-solution interface, thereby causing the formation of cation vacancies at the former interface [32]. Therefore, if the concentration of Cl^- is high, voids are known to form at the Ni-film interface. Growth of such voids leads to localized collapse of the passive film, leading to the formation of pits with selective dissolution of Ni, on the basis of a mechanism proposed by Ali and Ambrose [26]. Such a mechanism has been proposed to be operative in the bulk Ni-Cu alloys such as Monel-400. However, in the nanocrystalline alloys, pitting resistance is expected to be enhanced due to large grain boundary area fraction, as discussed above. The mechanism of pitting as mentioned above appears to be operative for the investigated $Ni_{90}Cu_{10}$ alloy, as suggested by the surface pits observed in Fig. 4 b.

The presence of TiN grains in the Ni-TiN nanocomposites lowers the exposed metallic area on the surface, which in turn improves the corrosion resistance. The results of the present study have confirmed that the presence of TiN grains play a major role in improving the corrosion resistance. The following mechanisms may be proposed to explain the enhancement of corrosion resistance due to the presence of TiN as reinforcement. Firstly, formation of TiO_2 on the surface of nanocomposite thin films during corrosion process protects the surface of films from further degradation. In this manner, the TiN grains become inert to further corrosive attack, and act as physical barriers for penetration of Cl^-. Secondly, dispersed TiN grains in the Ni matrix leads to the formation of many corrosion microcells where metallic Ni acts as anode and nanosize-TiN grains act as cathode, because of the more positive the standard potential for TiN as compared to Ni [33, 34]. These corrosion micro-cells smoothen the process of anodic polarization. Therefore, localized corrosion is inhibited due to the presence of nanosize-TiN grains. Thirdly, because the Ni-matrix grain size is also restricted in the presence of uniformly dispersed TiN particles, corrosion is observed to take more uniformly which leads to retardation in pitting corrosion.

5. Conclusion

Nanocrystalline Ni, $Ni_{90}Cu_{10}$, Ni-TiN and $Ni_{90}Cu_{10}$-TiN nanocomposite thin films have been successively processed by reactive magnetron co-sputtering with the grain sizes are around 13.6 ± 0.4 nm for Ni and 9.6 ± 0.3 nm for TiN. Nanocrystalline pure Ni is found to be susceptible to pitting corrosion in 3.5 g/l NaCl solution. Alloying of Ni with Cu is found to enhance the resistance to pitting corrosion. Further improvement in corrosion resistance is achieved on addition

of TiN due to formation of a passive film of TiO_2. Corrosion rate of the $Ni_{90}Cu_{10}$-TiN nanocomposite thin films is found to be (0.08×10^{-2} mm/yr), which is significantly less than the corrosion rate of pure nanocrystalline Ni (1.67×10^{-2} mm/yr).

Acknowledgement. The author is thankful to Indian Institute of Technology, Kharagpur, for their supports.

References

1. A. M. El-Sherik, U. Erb, G. Palumbo, K. T. Aust. Scripta Metall. Mater. 27 (9), 1185 (1992). Crossref
2. L. Benea, P. L. Bonora, A. Borello, S. Martelli. Wear. 249, 995 (2002). Crossref
3. H. Ferkel, B. Mueller, W. Riehemann. Mater. Sci. Eng. A. 234, 474 (1997). Crossref
4. P. Gyftou, E. A. Pavlatou, N. Spyrellis. Appl. Surf. Sci. 254, 5910 (2008). Crossref
5. M. R. Vaezi, S. K. Sadrnezhaad, L. Nikzad. Coll. Surf. A: Physicochem. Eng. Aspects. 315, 176 (2008). Crossref
6. A. Moller, H. Hahn. Nanostruct. Mater. 12, 259 (1999). Crossref
7. P. M. Vereecken, I. Shao, P. C. Searson. J. Electrochem. Soc. 147 (7), 2572 (2002). Crossref
8. X. Zhu, C. Cai, G. Zheng, Z. Zhang, J. Li. Trans. Nonferrous Met. Soc. China. 21, 2216 (2011). Crossref
9. C. T. J. Low, R. G. A. Wills, F. C. Walsh. Surf. Coat. Tech. 201, 371 (2006). Crossref
10. L. Liu, Y. Li, F. Wang. Electrochim. Acta. 52, 7193 (2007). Crossref
11. K. Bobzin. CIRP J. Manuf. Sci. Techn. 18, 1 (2017). Crossref
12. J. Yi, S. Chen, K. Chen, Y. Xu, Q. Chen, C. Zhu, L. Liu. Ceram. Int. 45, 474 (2019). Crossref
13. R. Dedoncker, P. Djemia, G. Radnóczi, F. Tétard, L. Belliard, G. Abadias, N. Martin, D. Depla. J. Alloy. Compd. 769, 881 (2018). Crossref
14. P. Vlcak, J. Fojt, Z. Weiss, J. Kopeček, V. Perina. Surf. Coatings Technol. 358, 144 (2019). Crossref
15. X. Chen, K. Liu, W. Guo, N. Gangil, A. N. Siddiquee, S. Konovalov. Rapid Prototyping Journal. 25 (8), 1421 (2019). Crossref
16. K. C. Chang, J. R. Zhao, F. Y. Hung. Metals. 11 (1), 87 (2021). Crossref
17. N. Gangil, H. Nagar, R. Kumar, D. Singh. Materials Today: Proceedings. 33, 378 (2020). Crossref
18. S. Balathandan, S. K. Seshadri. Metal. Finish. 92, 49 (1994).
19. M. Kumar, R. Mitra. Thin Solid Films. 624, 70 (2017). Crossref
20. M. Kumar, R. Mitra. Surf. Coat. Technol. 251, 239 (2014). Crossref
21. M. Kumar, S. Mishra, R. Mitra. Surf. Coat. Technol. 228, 100 (2013). Crossref
22. B. P. Sahu, M. Ray, R. Mitra. Materials Characterization. 169, 110604 (2020). Crossref
23. B. D. Cullity. Elements of X-Ray Diffraction, Second. Addison-Wesley Publishing Company, Inc. (1978)
24. M. Stern, A. L. Geary. J. Electro. Soci. 104, 56 (1957). Crossref
25. M. Stern. Corrosion. 14, 440 (1958).
26. J. A. Ali, J. R. Ambrose. Corrosion Science. 33, 1147 (1992). Crossref
27. K. Banerjee, U. K. Chatterjee. Scripta Met. 44, 213 (2001). Crossref
28. M. R. Zamanzad-Ghavidel, K. Raeissi, A. Saatchi. Materials Letters. 63, 1807 (2009). Crossref
29. T. Tukuda, M. B. Ives. Corrosion Science. 11, 297 (1971). Crossref
30. L. E. Eiselstein, B. C. Syrett, S. S. Wing, R. D. Caligiuri. Corrosion Science. 23 (3), 223 (1983). Crossref
31. E. M. Sherif, A. A. Almajid, A. K. Bairamov, E. Al-Zahrani. Int. J. Electrochem. Sci. 6, 5430 (2011).
32. V. K. Gouda, I. Z. Selim, A. A. Khedr, A. M. Fathi. J. Mater. Sci. Technol. 15, 208 (1999).
33. Q. Feng, T. Li, H. Teng, X. Zhang, Y. Zhang, C. Liu, J. Jin. Surf. Coat. Technol. 202, 4137 (2008). Crossref
34. X. H. Chen, C. S. Chen, H. N. Xiao, F. Q. Cheng, G. Zhang, G. J. Yi. Surf. Coat. Technol. 191, 351 (2005). Crossref